Metabarcoding and Metagenomics 6: 101–115 DOI 10.3897/mbmg.6.79208

Research Article

Comparative metagenomics of phytoplankton blooms after nutrient enrichment of oligotrophic marine waters

John K. Pearman[1,2], **Laura Casas**[2,3], **Craig Michell**[2,4], **Naroa Aldanondo**[2,5], **Nazia Mojib**[2,6], **Karie Holtermann**[2,7], **Ioannis Georgakakis**[2], **Joao Curdia**[2], **Susana Carvalho**[2], **Amr Gusti**[2], **Xabier Irigoien**[2,5,8]

1 *Cawthron Institute, Coastal and Freshwater Group, 98 Halifax Street East, Nelson, 7010, New Zealand*

2 *King Abdullah University of Science and Technology (KAUST), Red Sea Research Center, Thuwal, 23955-6900 Saudi Arabia*

3 *Institute of Marine Research (IIM-CSIC), Vigo, Spain*

4 *University of Eastern Finland, Department of Environmental and Biological Sciences, Yliopistokatu 7, Joensuu, 80101, Finland*

5 *AZTI – BRTA, Marine Research, Herrera Kaia, Portualdea z/g – 20110 Pasaia (Gipuzkoa), Spain*

6 *Spelman College, 350 Spelman Lane, S.W., Atlanta, GA 30314-4399, USA*

7 *City of Unalaska, P.O. Box 610, Unalaska, AK 99685, USA*

8 *IKERBASQUE, Basque Foundation for Science, Bilbao, Spain*

Corresponding author: John K. Pearman (john.pearman@cawthron.org.nz)

Academic editor: Uwe John | **Received** 11 December 2021 | **Accepted** 30 March 2022 | **Published** 12 April 2022

Abstract

Increasing anthropogenic pressures on the coastal marine environments impact these ecosystems via a variety of mechanisms including nutrient loading, leading to eutrophication and increases in algal blooms. Here, we use a metagenomics approach to assess the taxonomic and functional changes of the microbial community throughout a nutrient enriched mesocosm phytoplankton bloom. We tested four different nutrient treatments consisting of either nitrate and phosphate or nitrate, phosphate and silicate, administered on the first day or continuously for the first two weeks of the experiment. Our results show a shift in the taxonomic composition of the community over time that is dependent on the nutrient addition regime. Significant differences in the functional potential of the communities were detected, with an interaction between bloom period (pre-bloom, bloom and post-bloom) and nutrient treatment ($p = 0.004$). A sharp drop in functional similarity was observed in the first week in all treatments and after 20 days had not returned to pre-bloom levels. Changes within energy metabolism pathways showed a remarkable enrichment of the dissimilatory nitrate reduction pathway in the post-bloom period. Eukaryotic oxidative phosphorylation and photosynthetic antenna proteins were more abundant during the bloom, especially in the continuous treatment with silicate. Our results suggest that continuous (i.e. chronic) nutrient enrichment has a larger effect on the functioning of marine systems compared to a single (i.e acute) addition. A deep understanding of the functional and taxonomic shifts in the community during blooms is essential to reverse or mitigate human impacts on coastal environments.

Key Words

algal blooms, eutrophication, metagenomics, nutrient enrichment

Introduction

Ecological and biogeochemical processes in the marine system are driven by a diverse assortment of microbial organisms including members from the kingdoms Archaea, Bacteria and Eukarya. Microbial plankton are responsible for a variety of processes, including carbon fixation (Strom 2008; Jardillier et al. 2010), biogeochemical cycling (Falkowski et al. 2008; Strom 2008) and the transfer of energy between trophic levels (Weisse 1989). The biogeochemical cycling is dependent on the functional capacities of the community to cycle different elements (Louca et al. 2016).

Copyright *John K. Pearman et al.* This is an open access article distributed under the terms of the Creative Commons Attribution License (CC BY 4.0), which permits unrestricted use, distribution, and reproduction in any medium, provided the original author and source are credited.

Despite the importance of microbial organisms to the functioning of the marine system, the inherent difficulty to understand what controls a complex system with multiple connections (Huisman and Weissing 1999) has limited our understanding of the mechanisms organising microbial plankton communities. With the advent of high throughput sequencing technologies, there has been an increased understanding of the marine microbial community. Studies have primarily looked at changes in the taxonomy of the organisms contributing to the community and relating them to changes in the environment (Fuller et al. 2006; Gilbert et al. 2012; Massana et al. 2015, e.g. de Vargas et al. 2015; Pearman et al. 2016b, 2017). However, more recently, investigations involving deep sequencing the genes of these marine communities (functional potential) have increased with studies revealing a vast wealth of novel genes (Yooseph et al. 2007; Sunagawa et al. 2015; Duarte et al. 2020). Global expeditions, such as the Global Ocean Survey (Yooseph et al. 2007), Tara Oceans (Sunagawa et al. 2015) and Malaspina 2010 Circumnavigation (Acinas et al. 2021), have provided insight into spatial patterns in the metabolism of marine microbes on a worldwide scale, while seasonal patterns have been shown during temporal studies (Biller et al. 2018; Yoshitake et al. 2021).

Human population growth has resulted in the increased development of coastal regions leading to greater anthropogenic pressures on the coastal marine environments. One of the consequences of the increased development of the coastal zone is the higher discharge of anthropogenically related material into the marine environment. This can have an impact on the ecosystem via a variety of mechanisms including increased nutrient loading (Malone and Newton 2020) and consequent eutrophic processes. For instance, higher nutrient loading can cause increased rates of primary production, changes in algal biomass and composition, reductions in transparency and loss of biodiversity (Smith 2006). Transient increases in the abundance of phytoplankton are referred to as blooms and are usually dominated by one or a few species (Irigoien et al. 2004). These blooms are increasing in frequency, with elevated nutrient availability being one of the principal drivers behind this pattern (Lancelot et al. 1987; Paerl 1988; Huppert et al. 2002; Beman et al. 2005). An understanding of how the functional potential of a microbial community changes during nutrient enrichment and the resulting blooms has received less attention, although differences have been shown between bloom microcosms and controls (Rinta-Kanto et al. 2012) and with deep water nutrient enrichment experiments (Shi et al. 2012). Further, metatranscriptomic approaches have also been used to highlight changes in the metabolic pathways related to dinoflagellate blooms (Gong et al. 2017).

Pearman et al. (2016a, 2016b, 2017), using a metabarcoding approach, showed that nutrient additions led to changes in the composition of the microbial community within the Red Sea microbial plankton communities. We undertook shotgun metagenomic sequencing at various time points throughout a nutrient-enriched mesocosm phytoplankton bloom to investigate the taxonomic and functional changes of the microbial community (Fig. 1). We hypothesised that: i) the metagenomic sequencing will show changes in the taxonomic profile of the microbial community amongst treatments and over time; ii) compared with the control, the treatments will have a different functional potential; and that iii) the functional potential will change during the bloom with the post-bloom functional potential returning to a similar state to that of the pre-bloom community.

Methods

Experimental design

Mesocosm bags of 8000 l (depth: 2.5 m) were placed in the harbour of King Abdullah University of Science and

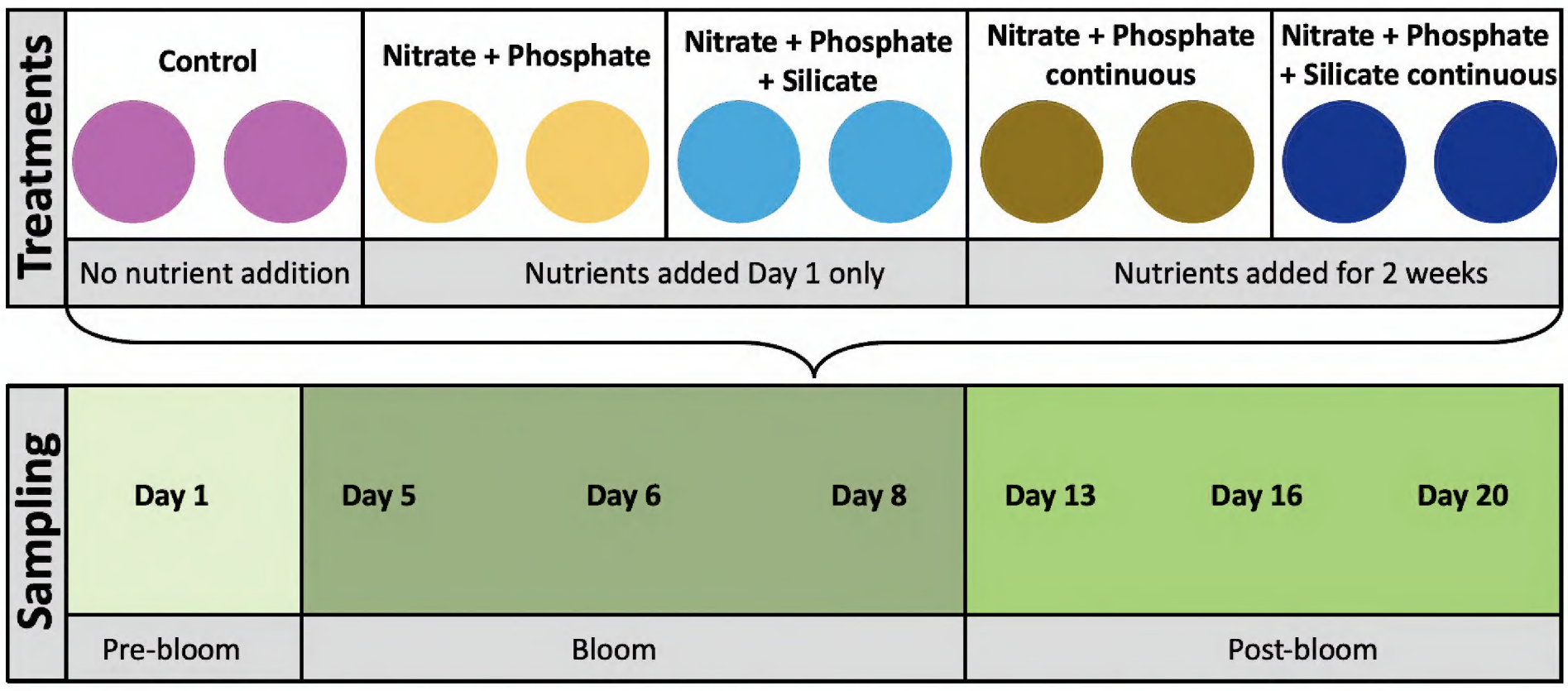

Figure 1. Framework showing the experimental set-up used to evaluate taxomic and functional changes of the microbial community throughout a nutrient-enriched mesocosm phytoplankton bloom.

Technology (KAUST), Thuwal, Saudi Arabia (22.304°N, 39.103°E). Sampling took place at solar noon over 20 days between the 27 January and 15 February 2013 (Suppl. material 6: Table S1). Mesocosm bags (8000 l) were subjected to five different treatments (2 replicates per treatment): 1) a single addition of nitrate ($NaNO_3$; 16 µM) and phosphate ($H_2NaPO_4.H_2O$; 1 µM), referred to as the NP treatment; 2) a single addition of nitrate (16 µM) and phosphate (1 µM) and silicate ($Na_2SiO_3.9H_2O$; 39 µM), referred to as the NPS treatment; 3) a continuous addition of nitrate (2 µM each day) and phosphate (0.12 µM each day) for the first two weeks, referred to as the NP.cont treatment; 4) a continuous addition of nitrate (2 µM each day), phosphate (0.12 µM each day) and silicate (3.75 µM each day) for the first two weeks, referred to as the NPS.cont treatment; and 5) control without nutrient additions. The ratios were adapted from those published by Wyman et al. (2000) and confirmed by a small scale microcosm experiment to show that the concentrations were able to induce a phytoplankton bloom (according to microscope counts).

Sample collection

A CTD profiler (Valeport Monitor CTD Profiler with an attached chlorophyll sensor) was used to measure daily profiles for temperature, salinity and fluorescence. The CTD was calibrated as per Millard and Yang (1993).

Samples for metagenomic analysis were collected in 20 l Niskin bottles and directly transferred to carboys for immediate filtration. To avoid destruction of delicate cells during filtration, peristaltic pumps at low speed (70 rpm) filtered approximately 4 l of seawater through a 0.2 µm hollow fibre CellTrap (Mem-Teq, UK). The concentrated cells within the CellTrap were eluted using 2 ml of filtered seawater (from the same sample) and the eluted cells were immediately frozen in liquid nitrogen and stored at -80 °C for later analysis.

Nutrient samples were collected as per the protocols of Brügmann and Kremling (1999) and Kremling and Brügmann (1999). In brief, water samples were filtered through 0.45 µm filters into acid washed (10% HCl acid overnight) sample bottles. Nitrate, nitrite and orthophosphate concentrations were assessed by means of Autoanalyser AAIII pentacanal BRAN-LUEBBE (with 10 nm optical path) using the protocols of Cauwet (1999) at AZTI Tecnalia. Ammonia was analysed by a SEAL Analytical AutoAnalyzer 3 at KAUST using the manufacturer's protocols.

Counts of total bacteria, the photosynthetic bacterial genus *Synechococcus*, photosynthetic picoeukaryotes and photosynthetic nanoeukaryotes were determined using a FACSVerse flow cytometer (Becton Dickinson, Belgium). Samples filtered through a 0.4 µm mesh were fixed in glutaraldehyde (2.5% final conc.) and flash frozen in liquid nitrogen. Cells were excited with a blue laser (488 nm wavelength) and red fluorescence emissions measured to discriminate the eukaryotic phytoplankton. Beads of size 1.002 µm (Polysciences, Europe) were added for size verification.

DNA extraction and metagenomic sequencing

DNA from the concentrated cells was extracted using a phenol:chloroform:isopropanol methodology combined with bead-beating, as described in Pearman et al. (2016a). Based on results described in Pearman et al. (2016a), samples targeting specific aspects of the bloom were selected for metagenomic sequencing. The pre-bloom sample was from day 1, while the peak bloom samples were taken on days 5, 6 and 8. Post-bloom samples were taken on days 13, 16 and 20 (note that samples for the control on day 16 are missing as they did not sequence). Paired end sequencing libraries (100 × 2 bp) were prepared following the manufacturer's protocols of the NEBNext Ultra DNA kit (#E7370L). After library construction, six samples per lane were sequenced on an Illumina HighSeq 2000 sequencer at the KAUST Biosciences Corelab (BCL). Raw sequences were stored in the National Centre for Biotechnology Information (NCBI) short read archive under the accession number: PRJNA395437.

Bioinformatics

PhiX sequences were removed from the samples using the bbduk.sh script (http://jgi.doe.gov/data-and-tools/bb-tools/) before processing using the software SqueezeMeta v.1.3.0 (Tamames and Puente-Sánchez 2019) with the co-assembly option. Firstly, sequences were trimmed with Trimmomatic v.0.39 (Bolger et al. 2014) to remove leading and trailing bases below a quality score of 20 and reads with an average per base quality of less than 30 over a 4 bp window. Assembly was undertaken using MEGAHIT (Li et al. 2015) with short contigs (< 500 bp) removed with prinseq (Schmieder and Edwards 2011). Reads for each sample were mapped to the assembly using Bowtie2 (Langmead and Salzberg 2012). Open reading frames (ORFs) were predicted using Prodigal (Hyatt et al. 2010) and similarity searches undertaken against the Kyoto Encyclopedia of Genes and Genomes (KEGG) (Kanehisa and Goto 2000) databases using DIAMOND with the options of evalue = 0.001 and id = 30 (Buchfink et al. 2015). For comparison across samples, the ORFs were normalised to reads per million (RPM). The RPM is calculated as reads per kilobase (RPK) / scaling factor, where the scaling factor is the sum of all RPK values divided by 10^6 reads. DIAMOND was used for taxonomic classification of the ORFs against the NCBI nr database with the SqueezeMeta default options evalue = 0.001 and id = 40.

To assess the taxonomic communities, open reading frames that had a phylogenetic classification to at least the kingdom level was used. The taxonomic composition was visualised in two ways. Firstly, to give an overview of the taxonomy in each treatment, ORFs were amalgamated at the class level and the percentage abundance calculated for each sample. The mean percentage abundance for each class was then calculated for each treatment. Secondly, after calculating the percentage abundance

for each class, the mean was calculated for each day in each treatment. The results were visualised in in ggplot2 v.3.3.5 (Wickham 2016).

The functional potential of the metagenomes was assessed at the level of KEGG Orthology ID (KO ID) with ORFs being amalgamated at this level. To assess the shared and unique KO IDs amongst treatments, all replicates within a treatment were merged together and then the presence/absences of KO IDs in the different treatments was assessed and visualised in the R package VennDiagram v.1.6.0 (Chen and Boutros 2011).

To test multivariate differences on the relative abundance (Bray Curtis) of KO IDs, a PERMANOVA was undertaken in the R package vegan v.2.7 (Oksanen et al. 2019) using the factors bloom period (3 levels; pre-bloom, bloom and post-bloom) and treatment (5 levels; Control, NP, NPS, NP.cont, NPS.cont) with an interaction term. To assess the association of environmental variables with the functional potential, a canonical correspondence analysis (CCA) was undertaken using the variables: ammonia, nitrate, phosphate, silicate concentrations and the counts of total bacteria, the photosynthetic prokaryote genus *Synechococcus*, picoeukaryotes and nano eukaryotes.

Raw read numbers were used to calculate differentially-abundant KO IDs using the DESeq2 package v.1.32.0 (Love et al. 2014) in R. KO IDs were considered differentially abundant if they had an adjusted (FDR) p-value < 0.05 in pairwise comparisons between the control and a treatment. Enriched metabolic pathways were identified by filtering the differentially-abundant KO IDs to only KEGG pathways involved in metabolism. These differentially-abundant KO IDs were used as the input for enrichment pathway analysis using clusterProfilier (Wu et al. 2021) with a pvalue cutoff of 0.05 and a minimum gene set size of 5. Pathway enrichment analysis was also undertaken, based on differentially-abundant KO IDs from pairwise comparisons between the control and the treatments for the bloom period, as well as the post-bloom period.

Temporal differences in functional differences were calculated, based on the average similarity (1 – Bray Curtis) of the relative abundance of the KO IDs between the control treatment and the nutrient additions for each sampling day. The temporal response of select metabolic pathways was investigated. The KEGG IDs that were used for this analysis are given in Suppl. material 7: Table S2. Average RPMs per pathway were calculated by summing all KEGG IDs within the pathway of interest for each sample and then finding the average either per day or per period.

Results

Reads, sequencing depth, contigs

A total 1,583,978,528 reads passed filtering and were used for SqueezeMeta. On average, 70% of a sample reads mapped to the contigs with an N50 of 1,606 bp. The number of reads mapped per sample is detailed in Suppl. material 8: Table S3. Overall, 2,979,235 ORFS were predicted using Prodigal (sample mean = 799,662, sd = 231,854; Suppl. material 8: Table S3 shows the numbers per sample). Of the almost three million ORFs, 40.4% could be annotated using the KEGG Orthology database and were attributed to 13,526 KO IDs (Suppl. material 8: Table S3 for the number of KEGG annotations per sample).

Taxonomic composition in treatments and over time

Proteobacteria dominated the metagenomic reads in all conditions (Suppl. material 1: Fig. S1) made up predominantly of Alphaproteobacteria (mean across treatments = 39.3%, sd = 9.3%) and Gammaproteobacteria (mean across treatments = 12.6%, sd = 6.4%). Cyanobacteria (mean across treatments = 14.9%, sd = 6.0%) and Flavobacteriia (mean across treatments = 5.6%, sd = 1.3%) also contributed substantially to the planktonic community. Eukaryotic taxa accounted for a higher proportion of the taxonomically-classified ORFs in the treatments with Bacillariophyceae accounting for a relative abundance of 7.0% in the NPS.cont treatment. Viruses of the class Caudoviricetes increased in relative abundance in the single addition treatments accounting for 4.7% in NP and 7.3% in NPS (Suppl. material 1: Fig. S1).

In the continuous treatments, relative abundances of Alphaproteobacteria were substantially higher during the bloom than in the pre-bloom period reaching an average of 59.4 ± 6.4% and 65.2 ± 7.0% in the NP.cont and NPS.cont, respectively (Fig. 2). The photosynthetic bacterial class Cyanobacteriia had the highest relative abundance in the pre-bloom period of the experiment, displaying a decrease in relative abundance during the bloom period, especially in the NP.cont and NPS.cont treatments where the class accounted for an average of only 1.5 ± 0.7% and 3.8 ± 3.0%, respectively (Fig. 2). Further declines were noted in the post-bloom period in the nutrient treatments with Cyanobacteriia accounting for less than 1% of the community in the NP.cont and NPS.cont treatments. The eukaryotic phytoplankton class Bacillariophyceae accounted for < 1% of the relative abundance, except during the bloom period of the NPS.cont treatment where it accounted for an average of 16.6 ± 3.4% of the community (Fig. 2). The bacteriophage Caudoviricetes increased in both the NP and NPS treatments during the bloom period with an average of 7.9 ± 2.5% and 17.7 ± 13.1% of the community, respectively before declining again towards the end of the experiment (Fig. 2). Proportional abundances per replicate are shown in Suppl. material 9: Table S4.

Functional composition

The majority (~92.5%) of the KO IDs were shared amongst all treatments (Suppl. material 2: Fig. S2). A total of 526 KO IDs were present in the nutrient enriched treatments, but absent from the control. The continuous treatments had the most unique sequences with thirty-one observed in

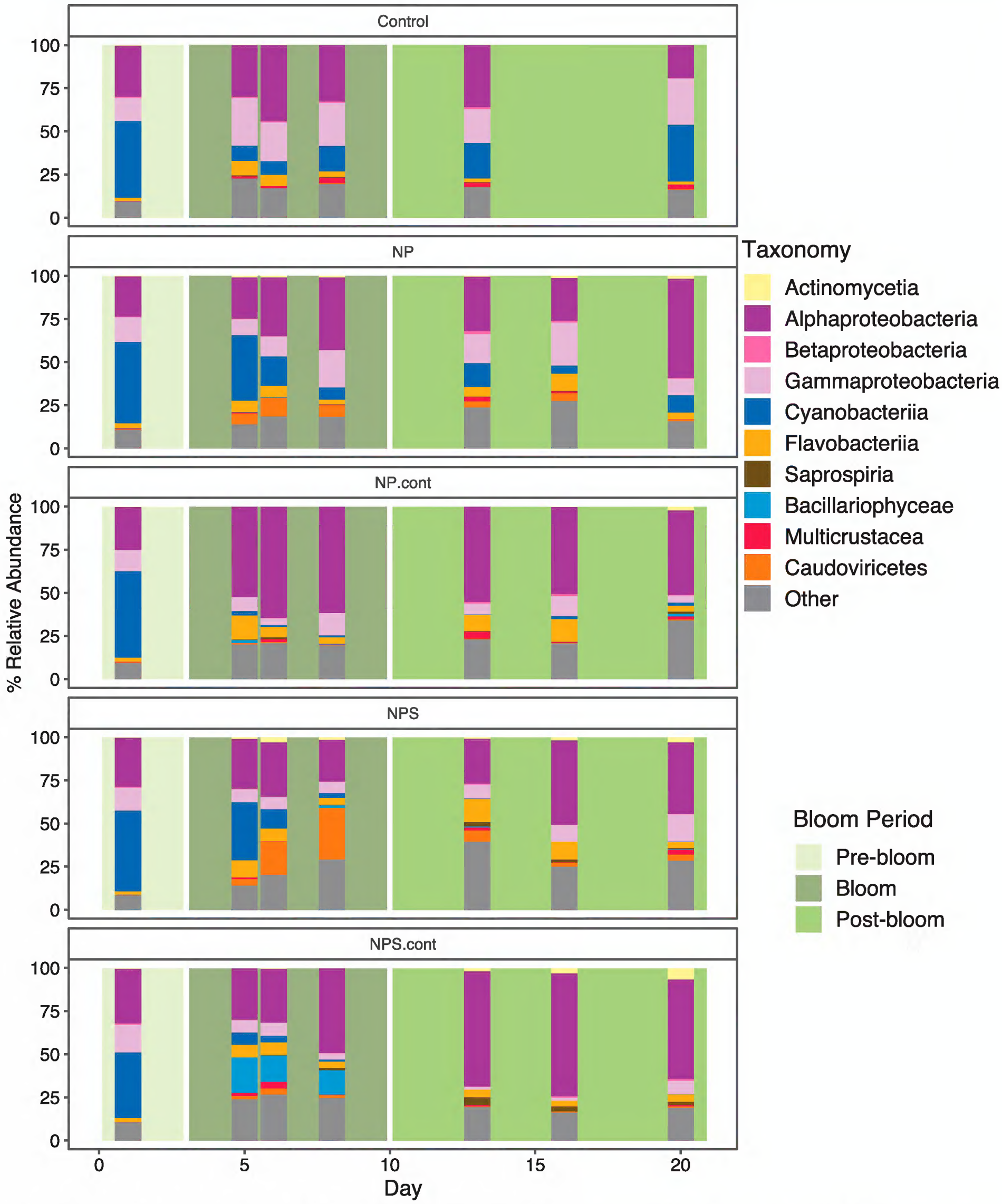

Figure 2. The relative abundance (%) of taxonomically-classified ORFs (only those with a kingdom level classification are depicted) at the phylum level by treatment and day of the experiment. Other includes taxa not classified at the phylum level and lower abundance phyla. NP = the single nitrate and phosphate addition; NP.cont = the continuous nitrate and phosphate addition; NPS = the single nitrate, phosphate and silicate addition; and NPS.cont = the continuous nitrate, phosphate and silicate (NPS.cont) addition.

the NP.cont treatment and thirty in the NPS.cont treatment. Mesocosms supplemented with silicate (NPS and NPS.cont) had a total of 75 unique KO IDs, while those mesocosms that were only enriched with nitrate and phosphate (NP and NP.cont) had 50 unique KO IDs.

Multivariate analysis indicated that there was a significant interaction between the variables treatment and bloom period in assessing the variation in the functional composition of the mesocosms (PERMANOVA; $F = 2.14$; $p = 0.004$). Canonical correspondence analysis

(Fig. 3A) showed that there was a cluster of samples from all treatments representing the start of the experiment associated with higher counts of *Synechococcus*. The end of the experiment was associated with higher concentrations of ammonia and total bacterial counts, while counts of nanoeukaryotes were correlated with the NPS.cont treatment. KO IDs related to photosynthesis (K08901, K08913) and carbon fixation (K18209, K01100) were shown to be associated with the bloom period of the NPS.cont treatment. A couple of sulphur cycles (K16951 and K17994) and nitrogen metabolism (K02591 and K15876) were associated with the post-bloom period of the NPS.cont treatment (Fig. 3B).

Differential abundance

In total, there were 5,789 KO IDs that had a differential abundance (padj < 0.05) between the control and at least one of the treatments (Fig. 4). In general, the differentially-abundant KO IDs had a higher abundance in the enriched treatments than the control. Of these 1,683 were related to metabolic pathways within KEGG. Comparisons between the control and the treatments showed that the continuous treatments had more enriched pathways compared to the single addition treatments with the NP treatment having no enriched pathways (Fig. 3). Biosynthesis of secondary metabolites was observed to be enriched in the NPS, NP.cont and NPS.cont treatments with nitrogen metabolism enriched in the continuous treatments (NP.cont and NPS.cont). Within the nitrogen metabolism pathway, KO IDs relating to the dissimilatory nitrate reduction to ammonia (DNRA) enzymes (NapAB and NrfAH) were differentially abundant in the NPS, NP.cont and NPS.cont treatments. Both the enzymes NarGHI and NirBD were differentially abundant in the NPS.cont treatment with the latter also significantly different in the NP.cont treatment. The first step, the conversion of nitrate to nitrite, in the assimilatory nitrate reduction was also significantly differentially abundant between the control and the NPS, NP.cont and NPS.cont treatments, although the second step showed no difference between the treatments and the control. The antenna protein pathway was enriched in the NPS.cont treatment compared to the control.

Temporal functional differences

The highest similarity between the nutrient treatments and the control was observed in the pre-bloom period with average similarity values ranging from 0.9 to 0.95. A decrease in similarity was observed in the bloom period with the largest declines observed in the treatments containing silicate with the NPS.cont treatment having a similarity value of 0.62 on day 6 and the NPS treatment having reached a low similarity value of 0.51 on day 8. The NPS.cont had an increase in similarity on day 8 before gradually declining during the post-bloom period, reaching an average similarity value compared to the control of 0.70 at the end of the experiment. For the NPS treatment, the post-bloom period showed an increase in similarity compared to the control with the average similarity being 0.72 on day 20. Regarding the NP.cont treatment, in general, similarity declined throughout the

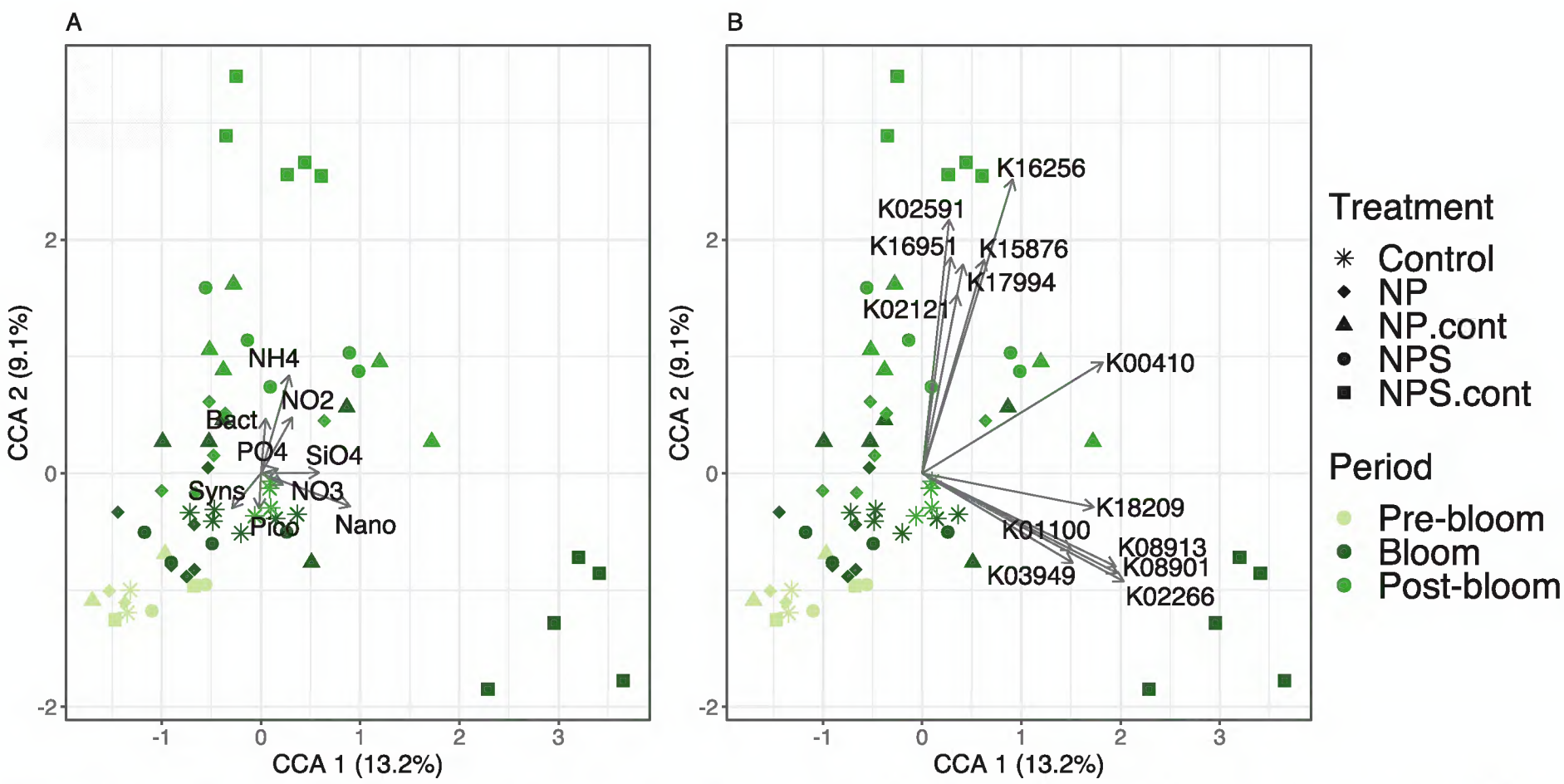

Figure 3. Canonical correspondence analysis, based on the ordination of the KO IDs and constrained by environmental variables (**A**) and some of the outermost KO IDs related to energy metabolism (**B**). Points are coloured by the bloom period with shapes indicating different nutrient treatments. NH_4 = Ammonium; NO_2; = Nitrite; SiO_4 = Silicate, PO_4 = Phosphate; Syns = Flow cytometry counts of Synechococcus; Pico = Flow cytometry counts of picoeukaryotes; Nano = Flow cytometry counts of nanoeukaryotes and Bact = Flow cytometry counts of total bacteria. NP = the single nitrate and phosphate addition; NP.cont = the continuous nitrate and phosphate addition; NPS = the single nitrate, phosphate and silicate addition; and NPS.cont = the continuous nitrate, phosphate and silicate (NPS.cont) addition.

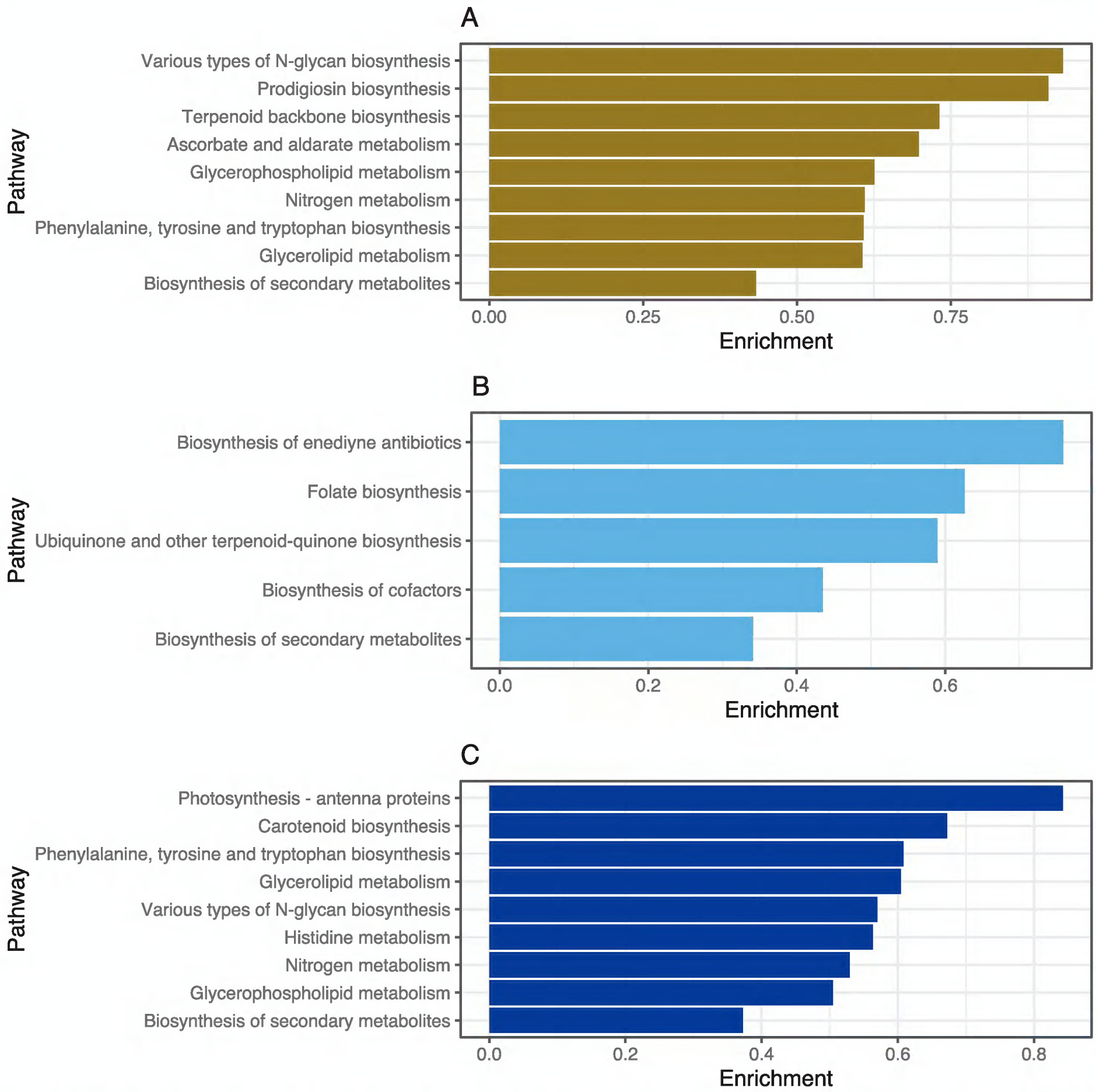

Figure 4. Enriched pathways in the nutrient treatments, based on significantly differentially-abundant KO IDs between the control and **A)** the continuous nitrate and phosphate (NP.cont) addition; **B)** the single nitrate, phosphate and silicate addition (NPS); and **C)** the continuous nitrate, phosphate and silicate (NPS.cont) addition.

experiment, reaching an average similarity value of 0.39 compared to the control at the end of the experiment. The NP treatment, after an initial decline and then recovery in similarity compared with the control in the bloom period, showed a shallow decline in similarity compared with the control over the post-bloom period, ending up with a similar average similarity (0.71) to the NPS and NPS.cont treatments (Fig. 5).

Focussing on changes within energy metabolism pathways differential abundance analysis followed by pathway enrichment analysis was undertaken comparing the bloom period in the control to the bloom period in the nutrient treatments. It showed that oxidative phosphorylation was enriched in the NPS.cont treatment, while nitrogen metabolism was enriched in the NP.cont treatment. Comparisons in the post-bloom period showed that the nitrogen metabolism pathway was enriched for all treatments, except the NP treatment.

Investigating the KO IDs in the nitrate reduction pathways showed a switch between assimilatory and dissimilatory nitrate reduction during the experiment, especially in the conversion of nitrite to ammonia (Fig. 6; Suppl. material 3: Fig. S3). At the beginning of the experiment there was a rapid drop off in nitrite reductase in the assimilatory pathway (Fig. 6 and Suppl. material 3: Fig. S3), while this enzyme increased over time in the NPS, NP.cont and NPS.cont treatments in the dissimilatory pathway (Fig. 6 and Suppl. material 3: Fig. S3).

Temporal differences were observed in the antenna proteins over the course of the experiment. Cyanobacterial

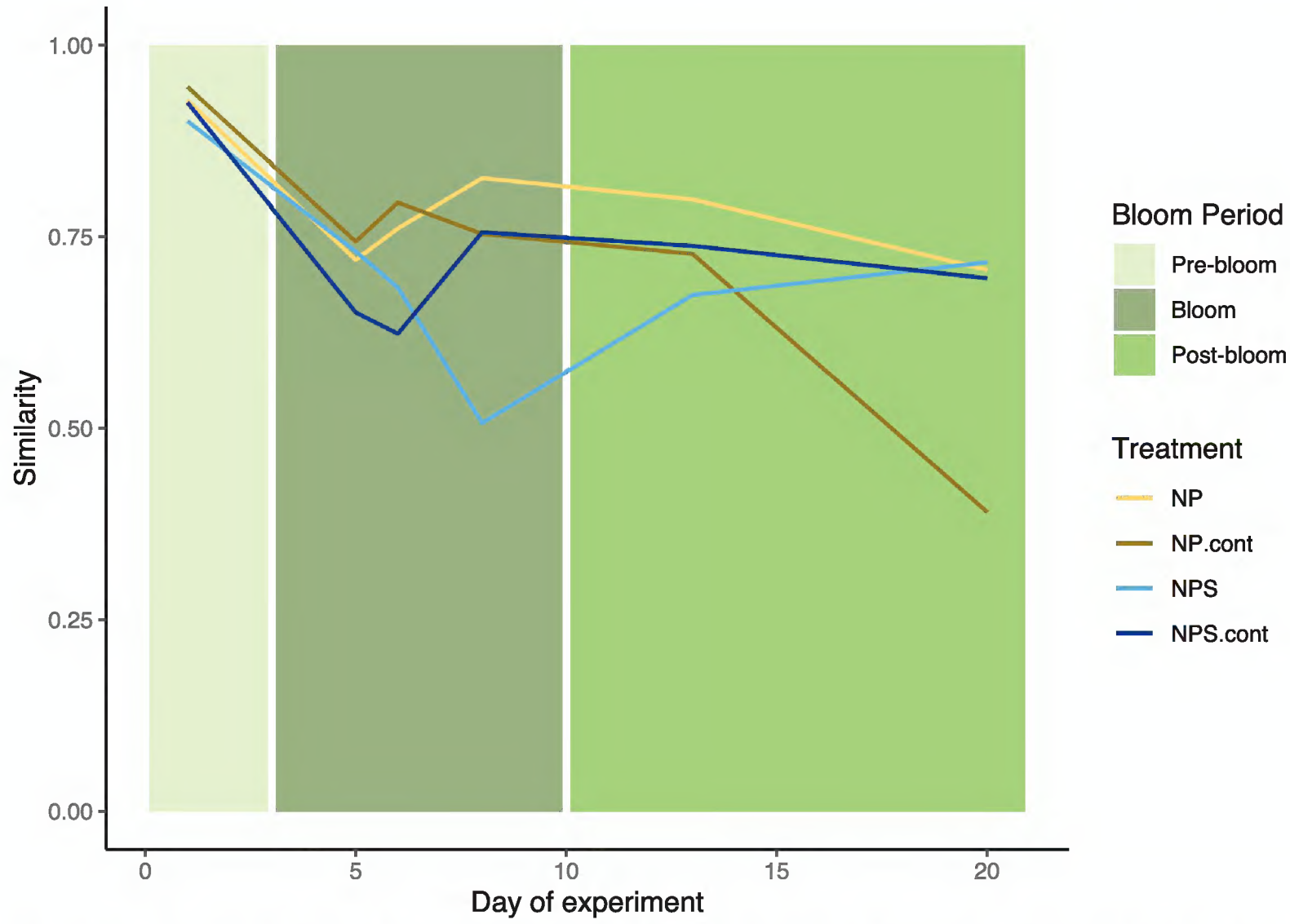

Figure 5. The average similarity based on 1 – Bray Curtis dissimilarity between the KO ID composition of the nutrient treatments compared to the control on each sampling day. Treatments are depicted in different colours. NP = single nitrate and phosphate addition; NPS = single nitrate, phosphate and silicate addition; NP.cont = continuous nitrate and phosphate addition; NPS.cont = continuous nitrate, phosphate and silicate addition.

antenna proteins (Allophycocyanin, Phycocyanin, Phycoerythrocyanin and Phycoerythrin) declined rapidly over the first 5–8 days, while the eukaryotic chlorophyll light harvesting complex increased, especially in the NPS.cont treatment, reaching a peak in the NPS.cont during the bloom on day 5 before declining again (Fig. 6; Suppl. material 4: Fig. S4).

Temporal dynamics within the oxidative phosphorylation pathway showed that the F type ATPase (Bacteria) was dominant in all treatments across time with no KO IDs differentially abundant for this ATPase (Fig. 6; Suppl. material 5: Fig. S5). KO IDs were differentially abundant in the NPS.cont for both the F type (Eukaryotes) and V type (Eukaryotes) with peaks on day 5 before declining in line with the increase in Bacillariophyta in the treatment during around day 5 (Fig. 6; Suppl. material 5: Fig. S5).

Discussion

Taxonomic changes

The development of coastal environments is having a substantial impact on marine communities. The addition of nutrients into the environment has been shown to affect the microbial community and has led to phytoplankton blooms (Lancelot et al. 1987; Paerl 1988). Metabarcoding results of the mesocosm samples used in this study showed that there was a distinct shift in the microbial communities in the continuous treatments compared with the control (Pearman et al. 2016a). This was especially evident in the NPS.cont treatment which saw a large diatom bloom. The taxonomic classification of the open reading frames, produced by the metagenomic sequencing, was in agreement in general with these results with Bacillariophyceae being more abundant in the NPS.cont treatment and especially during the bloom period. Proteobacteria were the dominant component in all treatments and had a substantial relative abundance throughout the experiment in agreement with the metabarcoding results (Pearman et al. 2016a) and is consistent with their distribution in marine systems (Eiler et al. 2009; West et al. 2016; Pearman et al. 2017). Cyanobacteria were substantial contributors at the beginning of the experiment, but their relative abundance and taxonomic composition changed over time with populations possibly controlled in a density dependent way by viruses which were especially prevalent in single addition treatments, as described for this dataset by Coello-Camba et al. (2020).

Metagenomic investigations are able to give a more holistic taxonomic view of the community incorporating taxa from viruses to eukaryotes without the potential of primer biases. This potentially gives a more robust understanding of the taxonomic composition of the community and, thus, providing better information for management decisions which rely on knowledge of taxonomic shifts. However, while the current sequencing effort was sufficient to detect the Bacillariophyta bloom, especially in the NPS.cont treatment, changes in other eukaryotic

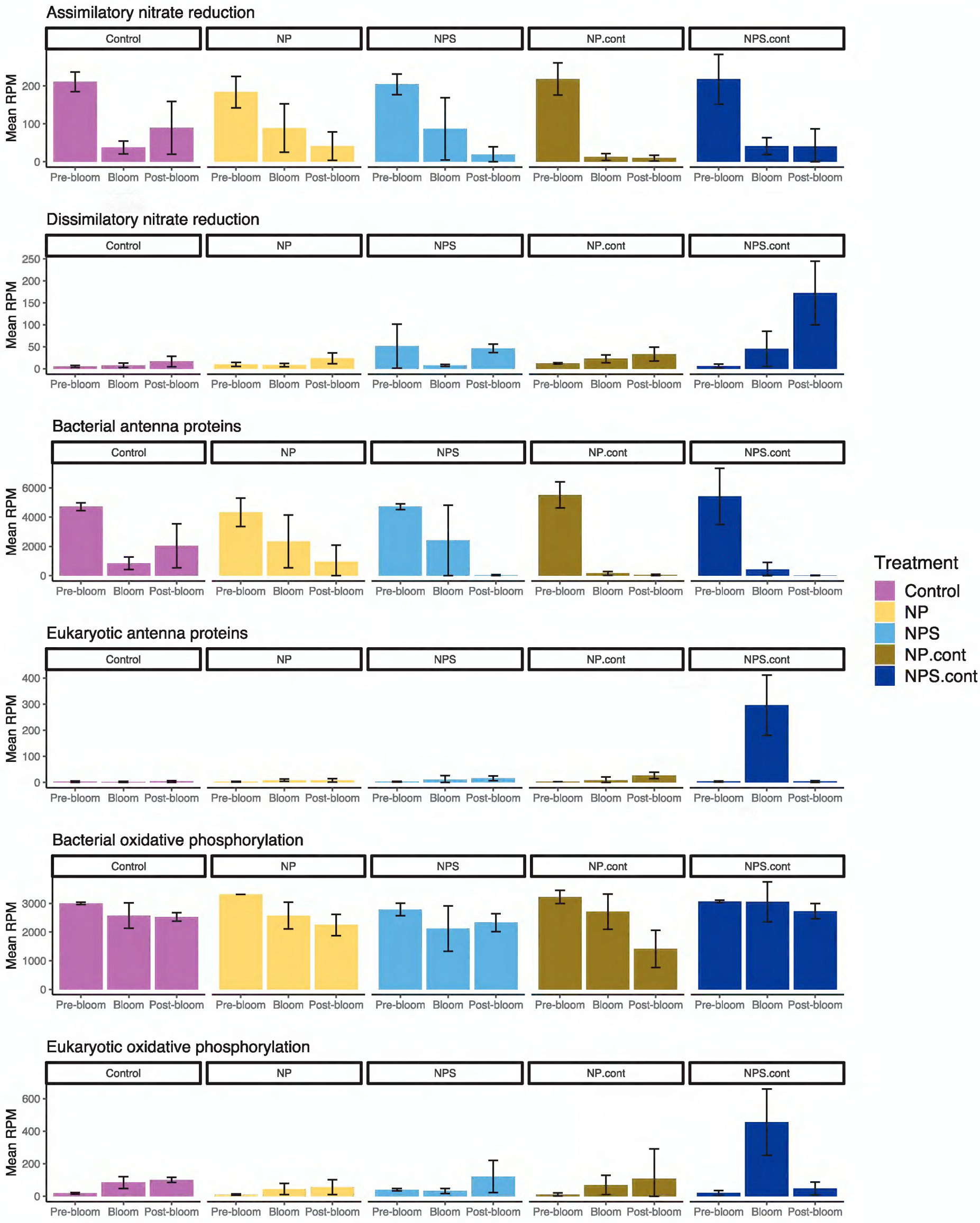

Figure 6. Mean reads per million (RPM) of selected pathways during the pre-bloom, bloom and post-bloom periods. NP = the single nitrate and phosphate addition; NP.cont = the continuous nitrate and phosphate addition; NPS = the single nitrate, phosphate and silicate addition; and NPS.cont = the continuous nitrate, phosphate and silicate (NPS.cont) addition.

groups were hard to determine. While Pearman et al. (2016a) were able to show differences in the protists using 18S rRNA metabarcoding, these were not detected in the metagenomics. Eukaryotes tend to be orders of magnitude less abundant than prokaryotes in the marine system (Jardillier et al. 2010) and, indeed, this was the case in the current experiment (Pearman et al. 2016a; Suppl. material 6: Table S1). Therefore, with a relatively low sequencing depth, these eukaryotic taxa would not be as comprehensively sequenced, limiting the ability for

contig assembly and, thus, analysis. To gain a fuller understanding of the eukaryotic dynamics during the bloom, a more substantial sequencing effort would be required.

Functional potential across treatments

Of the KO IDs that were annotated, over 90% of them were shared amongst all treatments. As a large proportion of the KO IDs are required for the cellular activity, the high proportion of shared KO IDs would be expected. While care should be taken due to the low number of replicates and, thus, lower statistical power, multivariate analysis showed that the addition of nutrients to the mesocosms and the progress of the bloom had a significant effect on the functional potential of the microbial community. This is further evidenced with approximately four percent of the KO IDs not being shared with the control, while 43% of the KO IDs were differentially abundant. The change in functional potential is in agreement with previous studies that have used metagenomic or transcriptomic approaches to assess phytoplankton blooms (Rinta-Kanto et al. 2012; Shi et al. 2012; Gong et al. 2017). Distinct differences were observed when comparing the effects of the treatments. The continuous treatments, which simulated a low-level chronic addition to the environment, showed more differentially-abundant KO IDs compared with the single addition treatments, which was akin to a high-level acute addition to the environment. This may indicate that the transformation of the additional nutrients into biomass was more efficient when persistent low concentrations of nutrients were added over time. This is supported by the fact that a higher number of enriched metabolic pathways in the continuous treatments were present.

The addition of silicate led to a more distinct community compared with the nutrient treatments containing only nitrogen and silicate. This can be explained by the greater increase in relative abundance of Bacillariophyta, which require silicate for growth (Egge and Aksnes 1992; Escaravage and Prins 2002), in these treatments and especially the NPS.cont treatment. This led to the differential abundance of eukaryotic genes, such as those involved in oxidative phosphorylation and the eukaryotic light harvesting complex which were not evident in the other treatments.

Temporal changes in functional potential

None of the treatments, including the control, had returned to a similar functional potential to that observed at the beginning of the experiment. However, with the exception of the NP.cont treatment, after initial drops in similarity compared to the control, there had been some recovery in similarity and stabilisation towards the end of the experiment. Different factors could explain why the community did not return to the same functional profile as before the bloom. Firstly, there may not have been sufficient time for the community to recover and this is especially true for the continuous treatments, which had nutrients supplied for the first couple of weeks and which brought about a larger and longer bloom. This could result in sufficient nutrients being recycled within the microbial loop (Azam et al. 1983; Fenchel 2008) preventing the return of the mesocosm to its pre-nutrient addition oligotrophic state. Secondly, although linked, is the fact that the mesocosms are semi-closed systems (only open to the air), so there is no water flow. Thus, organic matter or ammonia, for instance, are not removed from the system resulting in changes in the environmental niches present in the mesocosm. This could explain the almost total dominance of heterotrophic bacteria in the continuous and NPS treatments as they can rapidly utilise the organic matter (Obernosterer et al. 2008). Furthermore, as the mesocosms were open to the air, processes, such as evaporation (increasing salinity) and the input of dust (through sand storms), would also alter the environment within the mesocosm and could explain why the control also differed temporally. Finally, there is also the possibility that, once knocked out of its equilibrium, the ecosystem will not necessarily return to its previous state, at least in terms of species composition in the short term (Benincà et al. 2008; Dakos et al. 2009).

Distinct temporal differences were noted in the temporal patterns of nitrate reduction. Assimilatory nitrate reduction was shown to decline early in the experiment, showing a pattern similar to that of the contribution of cyanobacteria to the community. Cyanobacteria have previously been shown to undertake assimilatory nitrate reduction (Flores et al. 2005). In addition, the relationship between the reduction of assimilatory nitrate reduction and cyanobacteria proportional abundance could suggest that these taxa are responsible for the majority of assimilatory nitrate reduction in the surface waters of the Red Sea. Furthermore, assimilatory nitrate reduction is repressed by ammonia (Mohan and Cole 2007), which increased during the experiment. In contrast, dissimilatory nitrate reduction is not repressed by the increase in ammonia and was observed to increase throughout the experiment with KO IDs related to this pathway observed to be differentially abundant in the continuous nutrient treatments and especially the NPS.cont treatment. This process reduces nitrate to ammonia, recycling the fixed N in the system and is in competition with denitrification for free nitrate (van den Berg et al. 2015; Broman et al. 2021). Dissimilatory nitrate reduction requires anoxic conditions and has previously been described to happen in cyanobacterial aggregates (Klawonn et al. 2015). This could explain the increase of this process towards the end of the current experiment as the breakdown of the bloom creates anoxic micro-niches where dissimilatory nitrate reduction can occur and recycle the N within the system. Broman et al. (2021) suggested that approximately a fifth of the nitrate pool is recycled by dissimilatory nitrate reduction and has the potential to sustain algal proliferation and enhance eutrophication.

Differences were also observed in the temporal dynamics of the antenna proteins present in the mesocosms and highlights a shift in the taxa contributing to primary

production with nutrient enrichment. The prokaryotic antenna proteins (allophycocyanin, phycoerythrocyanin, phycocyanin and phycoerythrin) declined in line with the drop in the proportion of the community related to cyanobacteria. The eukaryotic light harvesting complexes increased especially in the NPS.cont treatment in line with the increase in Bacillariophyta within the community, reinforcing the results showing the shifts in the photosynthetic community with additional nutrients. Similarly, changes in the oxidative phosphorylation enzymes were noted with the shift in community with an increase in the eukaryote F and V type ATPases being observed with the increase in Bacillariophyta in the community in the NPS.cont treatment.

The sampling methodology undertaken in this study allowed for a temporal investigation of the functions occurring before, during and after a nutrient-stimulated phytoplankton bloom. Understanding, the processes occurring in each stage of the bloom (e.g. changes in nitrate reduction) is vital to understand the mechanisms of a bloom progression. This knowledge could then be used in future monitoring or remediation processes to mitigate the impacts of anthropogenic impacts (Techtmann and Hazen 2016).

Conclusions

With increasing anthropogenic impact on coastal waters, it is vital to understand how the microbial community responds to environmental changes, such as nutrient addition. In this study, we show that the addition of nutrients led to both a taxonomic and functional response in the planktonic community with continuous (i.e. chronic) nutrient enrichment having a larger effect compared to a single (i.e. acute) addition. Temporal dynamics showed that, in the time frame of the experiment, communities had not returned to comparable similarity levels to those obtained in the control, with the exception of the NP treatment. Temporal dynamics in energy metabolism pathways and especially in nitrate reduction and photosynthetic antenna proteins were evident as the bloom progressed and the nutrient conditions in the bloom progressed. The demonstration that there were functional shifts in the community as well as taxonomic shifts can provide management agencies a better understanding of how to respond to anthropogenic impacts. Understanding the mechanisms of the processes occurring in the community has the potential to improve decisions to reverse or mitigate the impacts from human impacts of coastal environments (Techtmann and Hazen 2016).

Acknowledgements

The authors would like to thank all those who helped during the deployment and running of the mesocosm experiment. Additionally, the authors would like to thank Prof. Jean-Philippe Croué for allowing the flow cytometry samples to be analysed using his equipment and Dr. Tony Merle for processing the samples. This research was supported by baseline funding provided by KAUST to Prof. Xabier Irigoien. The authors declare no conflicts of interest. We would like to thank the editor and three reviewers for their input into improving the manuscript.

References

Acinas SG, Sánchez P, Salazar G, Cornejo-Castillo FM, Sebastián M, Logares R, Royo-Llonch M, Paoli L, Sunagawa S, Hingamp P, Ogata H, Lima-Mendez G, Roux S, González JM, Arrieta JM, Alam IS, Kamau A, Bowler C, Raes J, Pesant S, Bork P, Agustí S, Gojobori T, Vaqué D, Sullivan MB, Pedrós-Alió C, Massana R, Duarte CM, Gasol JM (2021) Deep ocean metagenomes provide insight into the metabolic architecture of bathypelagic microbial communities. Communications Biology 4(1): 1–15. https://doi.org/10.1038/s42003-021-02112-2

Azam F, Fenchel T, Field JG, Gray JS, Meyer-Reil LA, Thingstad F (1983) The ecological role of water-column microbes in the sea. Marine Ecology Progress Series 10: 257–263. https://doi.org/10.3354/meps010257

Beman JM, Arrigo KR, Matson PA (2005) Agricultural runoff fuels large phytoplankton blooms in vulnerable areas of the ocean. Nature 434(7030): 211–214. https://doi.org/10.1038/nature03370

Benincà E, Huisman J, Heerkloss R, Jöhnk KD, Branco P, Van Nes EH, Scheffer M, Ellner SP (2008) Chaos in a long-term experiment with a plankton community. Nature 451(7180): 822–825. https://doi.org/10.1038/nature06512

Biller SJ, Berube PM, Dooley K, Williams M, Satinsky BM, Hackl T, Hogle SL, Coe A, Bergauer K, Bouman HA, Browning TJ, De Corte D, Hassler C, Hulston D, Jacquot JE, Maas EW, Reinthaler T, Sintes E, Yokokawa T, Chisholm SW (2018) Marine microbial metagenomes sampled across space and time. Scientific Data 5(1): e180176. https://doi.org/10.1038/sdata.2018.176

Bolger AM, Lohse M, Usadel B (2014) Trimmomatic: A flexible trimmer for Illumina sequence data. Bioinformatics (Oxford, England) 30(15): 2114–2120. https://doi.org/10.1093/bioinformatics/btu170

Broman E, Zilius M, Samuiloviene A, Vybernaite-Lubiene I, Politi T, Klawonn I, Voss M, Nascimento FJA, Bonaglia S (2021) Active DNRA and denitrification in oxic hypereutrophic waters. Water Research 194: 116954. https://doi.org/10.1016/j.watres.2021.116954

Brügmann L, Kremling K (1999) Sampling. In: Grasshoff K, Kremling K, Ehrhardt M (Eds) Methods of Seawater Analysis. John Wiley & Sons, 1–25. https://doi.org/10.1002/9783527613984.ch1

Buchfink B, Xie C, Huson DH (2015) Fast and sensitive protein alignment using DIAMOND. Nature Methods 12(1): 59–60. https://doi.org/10.1038/nmeth.3176

Cauwet G (1999) Determination of dissolved organic carbon and nitrogen by high temperature combustion. In: Grasshoff K, Kremling K, Ehrhardt M (Eds) Methods of Seawater Analysis. John Wiley & Sons, 407–420. https://doi.org/10.1002/9783527613984.ch15

Chen H, Boutros PC (2011) VennDiagram: a package for the generation of highly-customizable Venn and Euler diagrams in R. BMC bioinformatics 12: e35. https://doi.org/10.1186/1471-2105-12-35

Coello-Camba A, Diaz-Rua R, Duarte CM, Irigoien X, Pearman JK, Alam IS, Agusti S (2020) Picocyanobacteria community and cyanophage infection responses to nutrient enrichment in a mesocosms experiment in oligotrophic waters. Frontiers in Microbiology 11: e1153. https://doi.org/10.3389/fmicb.2020.01153

Dakos V, Benincà E, van Nes EH, Philippart CJM, Scheffer M, Huisman J (2009) Interannual variability in species composition explained as seasonally entrained chaos. Proceedings. Biological Sciences 276(1669): 2871–2880. https://doi.org/10.1098/rspb.2009.0584

de Vargas C, Audic S, Henry N, Decelle J, Mahe F, Logares R, Lara E, Berney C, Le Bescot N, Probert I, Carmichael M, Poulain J, Romac S, Colin S, Aury J-M, Bittner L, Chaffron S, Dunthorn M, Engelen S, Flegontova O, Guidi L, Horak A, Jaillon O, Lima-Mendez G, Lukes J, Malviya S, Morard R, Mulot M, Scalco E, Siano R, Vincent F, Zingone A, Dimier C, Picheral M, Searson S, Kandels-Lewis S, Acinas SG, Bork P, Bowler C, Gorsky G, Grimsley N, Hingamp P, Iudicone D, Not F, Ogata H, Pesant S, Raes J, Sieracki ME, Speich S, Stemmann L, Sunagawa S, Weissenbach J, Wincker P, Karsenti E, Tara Oceans C (2015) Eukaryotic plankton diversity in the sunlit ocean. Science 348(6237): 1261605. https://doi.org/10.1126/science.1261605

Duarte CM, Ngugi DK, Alam I, Pearman J, Kamau A, Eguiluz VM, Gojobori T, Acinas SG, Gasol JM, Bajic V, Irigoien X (2020) Sequencing effort dictates gene discovery in marine microbial metagenomes. Environmental Microbiology 22(11): 4589–4603. https://doi.org/10.1111/1462-2920.15182

Egge JK, Aksnes DL (1992) Silicate as regulating nutrient in phytoplankton competition. Marine Ecology Progress Series 83: 281–289. https://doi.org/10.3354/meps083281

Eiler A, Hayakawa DH, Church MJ, Karl DM, Rappe MS (2009) Dynamics of the SAR11 bacterioplankton lineage in relation to environmental conditions in the oligotrophic North Pacific subtropical gyre. Environmental Microbiology 11(9): 2291–2300. https://doi.org/10.1111/j.1462-2920.2009.01954.x

Escaravage V, Prins TC (2002) Silicate availability, vertical mixing and grazing control of phytoplankton blooms in mesocosms. Sustainable increase of marine harvesting: fundamental mechanisms and new concepts. Developments in Hydrobiology. Springer, Dordrecht, 33–48. https://doi.org/10.1007/978-94-017-3190-4_4

Falkowski PG, Fenchel T, DeLong EF (2008) The microbial engines that drive Earth's biogeochemical cycles. Science 320(5879): 1034–1039. https://doi.org/10.1126/science.1153213

Fenchel T (2008) The microbial loop – 25 years later. Journal of Experimental Marine Biology and Ecology 366(1–2): 99–103. https://doi.org/10.1016/j.jembe.2008.07.013

Flores E, Frías JE, Rubio LM, Herrero A (2005) Photosynthetic nitrate assimilation in cyanobacteria. Photosynthesis Research 83(2): 117–133. https://doi.org/10.1007/s11120-004-5830-9

Fuller NJ, Tarran GA, Cummings DG, Woodward EMS, Orcutt KM, Yallop M, Le Gall F, Scanlan DJ (2006) Molecular analysis of photosynthetic picoeukaryote community structure along an Arabian Sea transect. Limnology and Oceanography 51(6): 2502–2514. https://doi.org/10.4319/lo.2006.51.6.2502

Gilbert JA, Steele JA, Caporaso JG, Steinbruck L, Reeder J, Temperton B, Huse S, McHardy AC, Knight R, Joint I, Somerfield P, Fuhrman JA, Field D (2012) Defining seasonal marine microbial community dynamics. The ISME Journal 6(2): 298–308. https://doi.org/10.1038/ismej.2011.107

Gong W, Browne J, Hall N, Schruth D, Paerl H, Marchetti A (2017) Molecular insights into a dinoflagellate bloom. The ISME Journal 11(2): 439–452. https://doi.org/10.1038/ismej.2016.129

Huisman J, Weissing FJ (1999) Biodiversity of plankton by species oscillations and chaos. Nature 402(6760): 407–410. https://doi.org/10.1038/46540

Huppert A, Blasius B, Stone L (2002) A model of phytoplankton blooms. American Naturalist 159(2): 156–171. https://doi.org/10.1086/324789

Hyatt D, Chen G-L, LoCascio PF, Land ML, Larimer FW, Hauser LJ (2010) Prodigal: Prokaryotic gene recognition and translation initiation site identification. BMC Bioinformatics 11(1): e119. https://doi.org/10.1186/1471-2105-11-119

Irigoien X, Huisman J, Harris RP (2004) Global biodiversity patterns of marine phytoplankton and zooplankton. Nature 429(6994): 863–867. https://doi.org/10.1038/nature02593

Jardillier L, Zubkov MV, Pearman J, Scanlan DJ (2010) Significant CO_2 fixation by small prymnesiophytes in the subtropical and tropical northeast Atlantic Ocean. The ISME Journal 4(9): 1180–1192. https://doi.org/10.1038/ismej.2010.36

Kanehisa M, Goto S (2000) KEGG: Kyoto Encyclopedia of Genes and Genomes. Nucleic Acids Research 28(1): 27–30. https://doi.org/10.1093/nar/28.1.27

Klawonn I, Bonaglia S, Brüchert V, Ploug H (2015) Aerobic and anaerobic nitrogen transformation processes in N_2-fixing cyanobacterial aggregates. The ISME Journal 9(6): 1456–1466. https://doi.org/10.1038/ismej.2014.232

Kremling K, Brügmann L (1999) Filtration and storage. In: Grasshoff K, Kremling K, Ehrhardt M (Eds) Methods of Seawater Analysis. John Wiley & Sons, 27–40. https://doi.org/10.1002/9783527613984.ch2

Lancelot C, Billen G, Sournia A, Weisse T, Colijn F, Veldhuis MJW, Davies A, Wassman P (1987) Phaeocystis blooms and nutrient enrichment in the continental coastal zones of the North Sea. Ambio 16: 38–46.

Langmead B, Salzberg SL (2012) Fast gapped-read alignment with Bowtie 2. Nature Methods 9(4): 357–359. https://doi.org/10.1038/nmeth.1923

Li D, Liu C-M, Luo R, Sadakane K, Lam T-W (2015) MEGAHIT: An ultra-fast single-node solution for large and complex metagenomics assembly via succinct de Bruijn graph. Bioinformatics (Oxford, England) 31(10): 1674–1676. https://doi.org/10.1093/bioinformatics/btv033

Louca S, Parfrey LW, Doebeli M (2016) Decoupling function and taxonomy in the global ocean microbiome. Science 353(6305): 1272–1277. https://doi.org/10.1126/science.aaf4507

Love M, Anders S, Huber W (2014) Differential analysis of count data–the DESeq2 package. Genome Biology 15: e550. https://doi.org/10.1186/s13059-014-0550-8

Malone TC, Newton A (2020) The globalization of cultural eutrophication in the coastal ocean: Causes and consequences. Frontiers in Marine Science 7: e670. https://doi.org/10.3389/fmars.2020.00670

Massana R, Gobet A, Audic S, Bass D, Bittner L, Boutte C, Chambouvet A, Christen R, Claverie J-M, Decelle J, Dolan JR, Dunthorn M, Edvardsen B, Forn I, Forster D, Guillou L, Jaillon O, Kooistra WHCF, Logares R, Mahe F, Not F, Ogata H, Pawlowski J, Pernice MC, Probert I, Romac S, Richards T, Santini S, Shalchian-Tabrizi K, Siano R, Simon N, Stoeck T, Vaulot D, Zingone A, de Vargas C (2015) Marine protist diversity in European coastal waters and

sediments as revealed by high-throughput sequencing. Environmental Microbiology 17(10): 4035–4049. https://doi.org/10.1111/1462-2920.12955

Millard RC, Yang K (1993) CTD calibration and processing methods used at Woods Hole Oceanographic Institution. Woods Hole Oceanographic Institution. Technical Report, 100 pp. https://doi.org/10.1575/1912/638

Mohan SB, Cole JA (2007) The dissimilatory reduction of nitrate to ammonia by anaerobic bacteria. In: Bothe H, Ferguson SJ, Newton WE (Eds) Biology of the Nitrogen Cycle. Elsevier, Amsterdam, 93–106. https://doi.org/10.1016/B978-044452857-5.50008-4

Obernosterer I, Christaki U, Lefèvre D, Catala P, Van Wambeke F, Lebaron P (2008) Rapid bacterial mineralization of organic carbon produced during a phytoplankton bloom induced by natural iron fertilization in the Southern Ocean. Deep-sea Research. Part II, Topical Studies in Oceanography 55(5–7): 777–789. https://doi.org/10.1016/j.dsr2.2007.12.005

Oksanen J, Kindt R, Legendre P, O'Hara B, Stevens MHH, Oksanen MJ, Suggests M (2007) The vegan package. Community ecology package 10: 631–637.

Paerl HW (1988) Nuisance phytoplankton blooms in coastal, estuarine, and inland waters1. Limnology and Oceanography 33(4part2): 823–843. https://doi.org/10.4319/lo.1988.33.4part2.0823

Pearman JK, Casas L, Merle T, Michell C, Irigoien X (2016a) Bacterial and protist community changes during a phytoplankton bloom. Limnology and Oceanography 61(1): 198–213. https://doi.org/10.1002/lno.10212

Pearman JK, Kurten S, Sarma YVB, Jones B, Carvalho S (2016b) Biodiversity patterns of plankton assemblages at the extremes of the Red Sea. FEMS Microbiology Ecology 92(3): fiw002. https://doi.org/10.1093/femsec/fiw002

Pearman JK, Ellis J, Irigoien X, Sarma YVB, Jones BH, Carvalho S (2017) Microbial planktonic communities in the Red Sea: High levels of spatial and temporal variability shaped by nutrient availability and turbulence. Scientific Reports 7(1): e6611. https://doi.org/10.1038/s41598-017-06928-z

Rinta-Kanto JM, Sun S, Sharma S, Kiene RP, Moran MA (2012) Bacterial community transcription patterns during a marine phytoplankton bloom. Environmental Microbiology 14(1): 228–239. https://doi.org/10.1111/j.1462-2920.2011.02602.x

Schmieder R, Edwards R (2011) Quality control and preprocessing of metagenomic datasets. Bioinformatics (Oxford, England) 27(6): 863–864. https://doi.org/10.1093/bioinformatics/btr026

Shi Y, McCarren J, DeLong EF (2012) Transcriptional responses of surface water marine microbial assemblages to deep-sea water amendment. Environmental Microbiology 14(1): 191–206. https://doi.org/10.1111/j.1462-2920.2011.02598.x

Smith VH (2006) Responses of estuarine and coastal marine phytoplankton to nitrogen and phosphorus enrichment. Limnology and Oceanography 51(1part2): 377–384. https://doi.org/10.4319/lo.2006.51.1_part_2.0377

Strom SL (2008) Microbial ecology of ocean biogeochemistry: A community perspective. Science 320(5879): 1043–1045. https://doi.org/10.1126/science.1153527

Sunagawa S, Coelho LP, Chaffron S, Kultima JR, Labadie K, Salazar G, Djahanschiri B, Zeller G, Mende DR, Alberti A, Cornejo-Castillo FM, Costea PI, Cruaud C, d'Ovidio F, Engelen S, Ferrera I, Gasol JM, Guidi L, Hildebrand F, Kokoszka F, Lepoivre C, Lima-Mendez G, Poulain J, Poulos BT, Royo-Llonch M, Sarmento H, Vieira-Silva S, Dimier C, Picheral M, Searson S, Kandels-Lewis S, Bowler C, de Vargas C, Gorsky G, Grimsley N, Hingamp P, Iudicone D, Jaillon O, Not F, Ogata H, Pesant S, Speich S, Stemmann L, Sullivan MB, Weissenbach J, Wincker P, Karsenti E, Raes J, Acinas SG, Bork P, Boss E, Bowler C, Follows M, Karp-Boss L, Krzic U, Reynaud EG, Sardet C, Sieracki M, Velayoudon D (2015) Structure and function of the global ocean microbiome. Science 348(6237): 1261359. https://doi.org/10.1126/science.1261359

Tamames J, Puente-Sánchez F (2019) SqueezeMeta, a highly portable, fully automatic metagenomic analysis pipeline. Frontiers in Microbiology 9: e3349. https://doi.org/10.3389/fmicb.2018.03349

Techtmann SM, Hazen TC (2016) Metagenomic applications in environmental monitoring and bioremediation. Journal of Industrial Microbiology & Biotechnology 43(10): 1345–1354. https://doi.org/10.1007/s10295-016-1809-8

van den Berg EM, van Dongen U, Abbas B, van Loosdrecht MC (2015) Enrichment of DNRA bacteria in a continuous culture. The ISME Journal 9(10): 2153–2161. https://doi.org/10.1038/ismej.2015.26

Weisse T (1989) The microbial loop in the Red Sea: Dynamics of pelagic bacteria and heterotrophic nanoflagellates. Marine Ecology Progress Series 55: 241–250. https://doi.org/10.3354/meps055241

West NJ, Lepere C de O, Manes C-L, Catala P, Scanlan DJ, Lebaron P (2016) Distinct spatial patterns of SAR11, SAR86, and Actinobacteria diversity along a transect in the ultra-oligotrophic South Pacific Ocean. Frontiers in Microbiology 7: e234. https://doi.org/10.3389/fmicb.2016.00234

Wickham H (2016) ggplot2: elegant graphics for data analysis. Springer. https://doi.org/10.1007/978-3-319-24277-4

Wu T, Hu E, Xu S, Chen M, Guo P, Dai Z, Feng T, Zhou L, Tang W, Zhan L, Fu X, Liu S, Bo X, Yu G (2021) clusterProfiler 4.0: A universal enrichment tool for interpreting omics data. The Innovation 2(3): 100141. https://doi.org/10.1016/j.xinn.2021.100141

Wyman M, Davies JT, Crawford DW, Purdie DA (2000) Molecular and physiological responses of two classes of marine chromophytic phytoplankton (Diatoms and prymnesiophytes) during the development of nutrient-stimulated blooms. Applied and Environmental Microbiology 66(6): 2349–2357. https://doi.org/10.1128/AEM.66.6.2349-2357.2000

Yooseph S, Sutton G, Rusch DB, Halpern AL, Williamson SJ, Remington K, Eisen JA, Heidelberg KB, Manning G, Li WZ, Jaroszewski L, Cieplak P, Miller CS, Li HY, Mashiyama ST, Joachimiak MP, van Belle C, Chandonia JM, Soergel DA, Zhai YF, Natarajan K, Lee S, Raphael BJ, Bafna V, Friedman R, Brenner SE, Godzik A, Eisenberg D, Dixon JE, Taylor SS, Strausberg RL, Frazier M, Venter JC (2007) The Sorcerer II Global Ocean Sampling expedition: Expanding the universe of protein families. PLOS Biology 5(3): e16. https://doi.org/10.1371/journal.pbio.0050016

Yoshitake K, Kimura G, Sakami T, Watanabe T, Taniuchi Y, Kakehi S, Kuwata A, Yamaguchi H, Kataoka T, Kawachi M, Ikeo K, Tan E, Igarashi Y, Ohtsubo M, Watabe S, Suzuki Y, Asakawa S, Ishino S, Tashiro K, Ishino Y, Kobayashi T, Mineta K, Gojobori T (2021) Development of a time-series shotgun metagenomics database for monitoring microbial communities at the Pacific coast of Japan. Scientific Reports 11(1): e12222. https://doi.org/10.1038/s41598-021-91615-3

Supplementary material 1
Figure S1
Author: John K. Pearman, Laura Casas, Craig Michell, Naroa Aldanondo, Nazia Mojib, Karie Holtermann, Ioannis Georgakakis, Joao Curdia, Susana Carvalho, Amr Gusti, Xabier Irigoien
Data type: Figure (pdf .file)
Explanation note: Relative abundance of open reading frames (ORFS) taxonomically classified at the phylum level (ORFs required annotation at least to the kingdom level). Only the top 15 taxa were shown.
Copyright notice: This dataset is made available under the Open Database License (http://opendatacommons.org/licenses/odbl/1.0/). The Open Database License (ODbL) is a license agreement intended to allow users to freely share, modify, and use this Dataset while maintaining this same freedom for others, provided that the original source and author(s) are credited.
Link: https://doi.org/10.3897/mbmg.6.79208.suppl1

Supplementary material 2
Figure S2
Author: John K. Pearman, Laura Casas, Craig Michell, Naroa Aldanondo, Nazia Mojib, Karie Holtermann, Ioannis Georgakakis, Joao Curdia, Susana Carvalho, Amr Gusti, Xabier Irigoien
Data type: Figure (pdf .file)
Explanation note: Venn diagram depicting the shared and unique KEGG IDs amongst nutrient treatments. NP = the single nitrate and phosphate addition; NP.cont = the continuous nitrate and phosphate addition; NPS = the single nitrate, phosphate and silicate addition; and NPS.cont = the continuous nitrate, phosphate and silicate (NPS.cont) addition.
Copyright notice: This dataset is made available under the Open Database License (http://opendatacommons.org/licenses/odbl/1.0/). The Open Database License (ODbL) is a license agreement intended to allow users to freely share, modify, and use this Dataset while maintaining this same freedom for others, provided that the original source and author(s) are credited.
Link: https://doi.org/10.3897/mbmg.6.79208.suppl2

Supplementary material 3
Figure S3
Author: John K. Pearman, Laura Casas, Craig Michell, Naroa Aldanondo, Nazia Mojib, Karie Holtermann, Ioannis Georgakakis, Joao Curdia, Susana Carvalho, Amr Gusti, Xabier Irigoien
Data type: Figure (pdf .file)
Explanation note: Changes in the abundance of enzymes (RPM = reads per million) involved in A) assimilatory nitrate reduction and B) dissimilatory nitrate reduction over time for the various treatments. NP = the single nitrate and phosphate addition; NP.cont = the continuous nitrate and phosphate addition; NPS = the single nitrate, phosphate and silicate addition; and NPS.cont = the continuous nitrate, phosphate and silicate (NPS.cont) addition.
Copyright notice: This dataset is made available under the Open Database License (http://opendatacommons.org/licenses/odbl/1.0/). The Open Database License (ODbL) is a license agreement intended to allow users to freely share, modify, and use this Dataset while maintaining this same freedom for others, provided that the original source and author(s) are credited.
Link: https://doi.org/10.3897/mbmg.6.79208.suppl3

Supplementary material 4
Figure S4
Author: John K. Pearman, Laura Casas, Craig Michell, Naroa Aldanondo, Nazia Mojib, Karie Holtermann, Ioannis Georgakakis, Joao Curdia, Susana Carvalho, Amr Gusti, Xabier Irigoien
Data type: Figure (pdf .file)
Explanation note: The changes in abundance (RPM = reads per million) of antenna proteins over time. AP = Allophycocyanin, PC = Phycocyanin, PEC = Phycoerythrocyanin, PE = Phycoerythrin and LHC = Light harvesting chlorophyll protein complex. NP = the single nitrate and phosphate addition; NP.cont = the continuous nitrate and phosphate addition; NPS = the single nitrate, phosphate and silicate addition; and NPS.cont = the continuous nitrate, phosphate and silicate (NPS.cont) addition.
Copyright notice: This dataset is made available under the Open Database License (http://opendatacommons.org/licenses/odbl/1.0/). The Open Database License (ODbL) is a license agreement intended to allow users to freely share, modify, and use this Dataset while maintaining this same freedom for others, provided that the original source and author(s) are credited.
Link: https://doi.org/10.3897/mbmg.6.79208.suppl4

Supplementary material 5
Figure S5
Author: John K. Pearman, Laura Casas, Craig Michell, Naroa Aldanondo, Nazia Mojib, Karie Holtermann, Ioannis Georgakakis, Joao Curdia, Susana Carvalho, Amr Gusti, Xabier Irigoien
Data type: Figure (pdf .file)
Explanation note: Temporal dynamics of oxidative phosphorylation related enzymes for each of the treatments. RPM = reads per million; NP = the single nitrate and phosphate addition; NP.cont = the continuous nitrate and phosphate addition; NPS = the single nitrate, phosphate and silicate addition; and NPS.cont = the continuous nitrate, phosphate and silicate (NPS.cont) addition.
Copyright notice: This dataset is made available under the Open Database License (http://opendatacommons.org/licenses/odbl/1.0/). The Open Database License (ODbL) is a license agreement intended to allow users to freely share, modify, and use this Dataset while maintaining this same freedom for others, provided that the original source and author(s) are credited.
Link: https://doi.org/10.3897/mbmg.6.79208.suppl5

Supplementary material 6
Table S1
Author: John K. Pearman, Laura Casas, Craig Michell, Naroa Aldanondo, Nazia Mojib, Karie Holtermann, Ioannis Georgakakis, Joao Curdia, Susana Carvalho, Amr Gusti, Xabier Irigoien
Data type: Table (xlsx. file)
Explanation note: Metadata of the samples taken during the mesocosm experiment.
Copyright notice: This dataset is made available under the Open Database License (http://opendatacommons.org/licenses/odbl/1.0/). The Open Database License (ODbL) is a license agreement intended to allow users to freely share, modify, and use this Dataset while maintaining this same freedom for others, provided that the original source and author(s) are credited.
Link: https://doi.org/10.3897/mbmg.6.79208.suppl6

Supplementary material 7
Table S2
Author: John K. Pearman, Laura Casas, Craig Michell, Naroa Aldanondo, Nazia Mojib, Karie Holtermann, Ioannis Georgakakis, Joao Curdia, Susana Carvalho, Amr Gusti, Xabier Irigoien
Data type: Table (xlsx. file)
Explanation note: KEGG IDs that were used in the analysis of temporal patterns of select metabolic pathways.
Copyright notice: This dataset is made available under the Open Database License (http://opendatacommons.org/licenses/odbl/1.0/). The Open Database License (ODbL) is a license agreement intended to allow users to freely share, modify, and use this Dataset while maintaining this same freedom for others, provided that the original source and author(s) are credited.
Link: https://doi.org/10.3897/mbmg.6.79208.suppl7

Supplementary material 8
Table S3
Author: John K. Pearman, Laura Casas, Craig Michell, Naroa Aldanondo, Nazia Mojib, Karie Holtermann, Ioannis Georgakakis, Joao Curdia, Susana Carvalho, Amr Gusti, Xabier Irigoien
Data type: Table (xlsx. file)
Explanation note: Sequencing, assembly and annotation results.
Copyright notice: This dataset is made available under the Open Database License (http://opendatacommons.org/licenses/odbl/1.0/). The Open Database License (ODbL) is a license agreement intended to allow users to freely share, modify, and use this Dataset while maintaining this same freedom for others, provided that the original source and author(s) are credited.
Link: https://doi.org/10.3897/mbmg.6.79208.suppl8

Supplementary material 9
Table S4
Author: John K. Pearman, Laura Casas, Craig Michell, Naroa Aldanondo, Nazia Mojib, Karie Holtermann, Ioannis Georgakakis, Joao Curdia, Susana Carvalho, Amr Gusti, Xabier Irigoien
Data type: Table (xlsx. file)
Explanation note: The percentage abundance per replicate of the top taxonomic classes per day and treatment.
Copyright notice: This dataset is made available under the Open Database License (http://opendatacommons.org/licenses/odbl/1.0/). The Open Database License (ODbL) is a license agreement intended to allow users to freely share, modify, and use this Dataset while maintaining this same freedom for others, provided that the original source and author(s) are credited.
Link: https://doi.org/10.3897/mbmg.6.79208.suppl9